International Journal of Impact Engineering 211 (2026) 105617

Contents lists available at ScienceDirect

International Journal of Impact Engineering

journal homepage: www.elsevier.com/locate/ijimpeng

Reliability-based evaluation of Cross-Laminated Timber (CLT) ballistic resistance for performance prediction and design

Juliet Swinea [a,*], Iris Tien [a], Peter Stynoski [b], Lauren K. Stewart [a]

[a] Department of Civil and Environmental Engineering, Georgia Institute of Technology, Atlanta, GA, USA
[b] US Army Engineer Research and Development Center (ERDC), Champaign, IL, USA

ARTICLE INFO

Keywords:
Cross-laminated timber (CLT)
Ballistics
Reliability
First-order second-moment (FOSM) method
Force protection design

ABSTRACT

Cross-laminated timber (CLT) is a promising sustainable building material for temporary and permanent military applications. Experimental research in the past decade informed design guidance for CLT components against blast loading and forced entry, but formal guidance for CLT systems under ballistic impact is not currently available partly due to inherent uncertainties affecting localized resistance. In this article, we investigate the impact of quasi-static wood material property variability on partial penetration ballistic resistance uncertainty by conducting 61 total ballistic impact experiments on an untested prominent structural species, Douglas Fir (DF). With the DF experimental results in combination with a leveraged CLT ballistic and material property database, we predict and characterize the ballistic resistance of any CLT panel using a defined single penetration depth equation and the computationally inexpensive reliability-based First-Order Second-Moment (FOSM) method. We use this approach to characterize and capture the inherent variability of CLT under ballistic impact, and represent resistance profiles as probabilistic distributions rather than single values. We apply the predictive method at different scales, from DF panel-specific single velocity estimates to full species partial penetration profiles. For each data grouping, the FOSM prediction fully captured within 95% confidence intervals the experimental dataset. Needing only two easily obtained wood material properties, the method provides accurate and robust predictions of the resistance of this variable material under dynamic localized loading. As a result, we argue predicted baseline resistance profiles considering inherent material variability can act as the informed starting point for decision makers to apply situation dependent design safety factors.

1. Introduction

Cross laminated timber (CLT) is an engineered wood product composed of stacked adhered lumber with alternating 90-degree orientation from layer to layer to reduce the effect of natural defects and introduce capacity in two-way action [1–3]. First developed in Europe in the 1990s, CLT serves as a sustainable and logistically advantageous building material. In the last two decades, the use of CLT and mass timber products in mid-rise structural applications has grown in popularity due to quick erection potential from component prefabrication and inherent lighter weights compared to typical building materials like concrete and steel [4–7]. CLT and mass timber systems are prime candidates for deployed military missions due their modularity, where components can be prefabricated, flat packed and shipped, erected on site, and later deconstructed and reused, leaving ground conditions unaltered [8–10]. However, the performance of CLT under ballistic impact is difficult to predict due to inherent uncertainties affecting localized resistance. To support the integration of CLT in force protection design guides, the research presented in this paper aims to predict and characterize the ballistic resistance of any CLT panel using reliability-based approaches, namely the computationally inexpensive First-Order Second-Moment (FOSM) method. Results show accurate and robust predictions of performance for this highly variable material under ballistic impact. As a result, we argue predicted baseline resistance profiles considering inherent material variability can act as the informed starting point for decision makers to apply situation dependent design safety factors.

1.1. CLT in force protection

Experimental research conducted by [10–20] have investigated the performance of CLT and multi-material layered timber composites

* Corresponding author.
E-mail address: jswinea3@gatech.edu (J. Swinea).

https://doi.org/10.1016/j.ijimpeng.2025.105617
Received 5 September 2025; Received in revised form 8 December 2025; Accepted 18 December 2025
Available online 19 December 2025

(coined Enhanced CLT or ECLT) against force protection threats, namely ballistic impact, blast explosion, and forced entry. Light-frame timber construction is rarely considered for protective design, so published work on wood mechanical response under high rate and localized loading is minimal [21]. Foundational large-scale live blast experimentation [22] along with shock tube testing [15] informed analysis guidance for CLT construction exposed to blast loading documented in PDC-TR 18–02 [11]. These organized efforts showed the viability of CLT structures subjected to General Service Administration (GSA) threat levels, focusing on flatwise bending elastic and plastic regimes to build single degree of freedom (SDOF) resistance functions for three, five, and seven ply CLT panels commercially sourced from Nordic Structures, DR Johnson, and SMARTLAM. Additional work by [13–15,20] looked at CLT dynamic boundary response and flatwise bending performance of CLT panels reinforced with steel plates. Although CLT structural response under far field blast loading is well understood and standardized for design, localized resistance under ballistic impact is not due to the inherent localized variability of wood as a natural material. To address this gap and limiter of CLT utilization in force protection applications, this paper uses material level quantified variability to predict ballistic resistance uncertainty, yielding CLT ballistic unfactored design curves encompassing intrinsic variability.

The limiting factor and driver for increased CLT thickness requirements is ballistic resistance. Wood is orders of magnitude less hard and dense than steel, fiber armoring composites, concrete or any typical protective building material [23]. Currently there is no formal design guidance for mass timber or specifically CLT under ballistic impact. However, design guidance for dimensional lumber was developed and defined in UFC 4–023–07 Design to Resist Direct Fire Weapons Effects where Eq. (1) gives the thickness of wood, T_w (in), necessary to resist perforation. The variables included in the equation are striking velocity, v (ft/s), weight of projectile, w (lbs), density of wood, ρ (lb/ft^3), diameter of projectile, D (in), and Janka hardness of the wood, H (lbs). Eq. (1) is a physics-based empirical design equation that includes projectile- and target-specific input variables with calibration coefficients.

$$T_w = 9837\left(\frac{v^{0.4113}w^{1.4897}}{\rho\left(\frac{\pi D^2}{4}\right)^{1.3596}H^{0.5414}}\right) \tag{1}$$

In the first ballistic evaluation of CLT, [17] experimentally tested spruce pine fir south (SPF-S) and southern yellow pine (SYP) CLT under ballistic impact to build partial and full penetration profiles. By building these profiles, [17] was able to assess the goodness of fit of prominent penetration models using sum of least squares optimization to determine fitting coefficients. A recalibrated UFC formulation fit the species dependent partial penetration datasets with the lowest cumulative error, and was therefore deemed the best model. Further, [18] showed that a single recalibrated UFC equation had slightly higher error when fitted to four unique partial penetration datasets, but could be utilized for design with an appropriate safety factor. The UFC formulation is advantageous because by including both target and projectile parameters, a generic form of the equation is feasible, and we can generate design curves for threat- and wood material property-specific inputs. Therefore, the UFC formulation is used as a basis for work in this study. However, the question then becomes, how do we quantify not only partial and full penetration design curves, but the inherent scatter around those curves due to characteristic material uncertainties of CLT? In this article, we aim to answer this question by applying predictive data analytic techniques to newly collected experimental data and a leveraged CLT ballistic and material property database to result in probabilistic characterization of CLT performance under ballistic impact.

1.2. Ballistic design considerations for wood

The structure of wood is inhomogeneous and anisotropic, resulting from the natural growth patterns of trees. Slow and fast growth periods correspond to higher and lower relative density regions represented by circumferential rings, and mechanical properties differ in three principal directions relative to the grain: longitudinal, transverse, and radial [24,25]. In addition to directional dependence, mechanical performance is affected by environmental and loading conditions, namely moisture content, temperature, biological decay, and load duration. This results in inherently variable material properties for a given species of wood, which makes it difficult to mechanically model with high fidelity. Nonetheless, we have historically utilized wood as a structural building material, with documented use dating back over 10,000 years [26].

It is convenient and typically appropriate to use average experimental values as representative for historical ballistic resistant materials like steel or fiber composites in analytical or numerical calculations [27,28]. The ballistic data presented in [17–19,29] shows significant scatter in resistance under constant high rate loading conditions, so when thinking about integration of wood products in force protection environments, designing structures with average resistance values will sometimes overpredict resistance, unacceptable in protective design. To truly represent the material, we need a way to predict not only average resistance for different wood species, but deviations around that average. With this type of representation, we can appropriately classify the material behavior as a distribution rather than a single value commonly seen for other materials in force protection and structural design.

In engineering problems, we often do not have the information required for explicit solutions, so we heavily rely on probability-based approximation techniques as prediction tools to inform limit state-based design such as load and resistance factor design (LRFD), foundational in structural engineering including wood design [24,30–34]. The complex problem outlined here encompasses an inherently variable system under localized dynamic loading. A goal is to predict the penetration performance of a CLT system by leveraging a simple reliability-based method involving a closed form physics-based empirically fit equation and experimentally collected material-specific input distributions. We present and evaluate the efficacy of the proposed approach, and with sensitivity analyses additionally investigate the influence of material properties (density and hardness) and their direct relationship on the ballistic resistance of CLT.

2. Formulation and theory

2.1. First-order second-moment (FOSM) method

Probability-based reliability methods are prominent in evaluating the reliability of a structural system for engineering design [35,36]. By considering the random nature of variables that affect the behavior of a structure, such as material properties, geometry, and loads, we can apply reliability-based design techniques to structural systems. The expected value or first-order moment of a random variable Y (μ(Y)) can be represented as a function of random variables $\mathbf{X}$, $Y = f(\mathbf{X})$, given by Eq. (2), where $p_{\mathbf{x}}$ is the joint probability density function (PDF) of $\mathbf{X}$. Further, the variance or second order moment of Y (Var(Y)) is given in Eq. (3).

$$\mu(Y) = \int_{-\infty}^{\infty} f(\boldsymbol{X})p_x(\boldsymbol{X})d\boldsymbol{X} \tag{2}$$

$$Var(Y) = \int_{-\infty}^{\infty} [f(\boldsymbol{X}) - \mu(Y)]^2 p_{\boldsymbol{X}}(\boldsymbol{X}) d\boldsymbol{X} \tag{3}$$

To use these equations, we must know p_X, which poses a challenge in many engineering applications where we must consider multiple random variables and their relative relationships, but we often cannot yet completely define individual variable PDFs and sometimes even explicit variable relationships. However, we can typically approximate mean and variance statistics with experimental sampling. When these statistics are available but PDFs are not, we can approximate the expected value and variance of a dependent output random variable (here the function of input random variables) with statistical methods. The FOSM method (synonymous with first-order Taylor series expansion) is a reliability-based approximation technique widely applied in engineering design [35,37,38]. For a continuous function with continuous derivatives, the Taylor series expansion of f(x) about c is given in Eq. (4), where the first-order expansion is given in Eq. (5) for $k = 1$.

$$\sum_{k=0}^{\infty} \frac{1}{k!} f^{(k)}(c)(x-c)^k \tag{4}$$

$$f(c) + f'(c)(x-c) \tag{5}$$

The expansion estimates an output value and variance using the first-order terms in a Taylor series around the mean of input random variables [37]. A computationally inexpensive tool, the FOSM method does not require defined PDF functions to describe random variables, and therefore we can simply predict the mean and variance of an output variable with the means and variances of input variables, which typically are available, related through an analytic expression. Of course, there are limitations to this method, especially when relationships between variables become highly nonlinear or the output variable distribution is nonnormal. Modifications to FOSM have been described, mainly accounting for more complex variable descriptions or when analytical expressions are not available [38,39]. However, FOSM remains a simple powerful tool for conducting reliability analyses, and the accuracy and robustness of this approach to predict probabilistic performance of CLT with inherent variabilities under ballistic impact is investigated in this work.

Here, we will apply the FOSM method to predict the partial penetration of a projectile into a CLT target. To start, we define a closed form equation and random variable means, variances, and correlations. We use the UFC formulation as the analytical function for depth of penetration (DOP) in Eq. (6), where the random variables included are striking velocity, v (ft/s), weight of projectile, w (lbs), density of wood, ρ (lb/ft^3), diameter of projectile, D (in), and Janka hardness of the wood, H (lbs). C1, a, b, c, and d are fitting coefficients based on least squares regression and are therefore constant values.

$$DOP = C1\left(\frac{v^a w^b}{\rho\left(\frac{\pi D^2}{4}\right)^c H^d}\right) = f(v,\ w,\ \rho,\ D,\ H) \tag{6}$$

Using this formulation, we formed a first-order Jacobian matrix J, which is the sensitivity or rate of change of the output variable, DOP, relative to each input random variable (Eq. (7)).

$$J = \left[\frac{\partial f}{\partial v}, \frac{\partial f}{\partial w}, \frac{\partial f}{\partial \rho}, \frac{\partial f}{\partial D}, \frac{\partial f}{\partial H}\right] \tag{7}$$

We can then calculate the predicted variance and subsequent standard deviation of DOP using Eqs. (8) and Eq. (9), with the Jacobian and covariance matrix Σ and mean and variance variable dependent inputs.

$$Var(DOP) = J(\mu_v, \mu_w, \mu_\rho, \mu_D, \mu_H) * \Sigma * J(\mu_v, \mu_w, \mu_\rho, \mu_D, \mu_H)^T \tag{8}$$

$$\sigma(DOP) = \sqrt{Var(DOP)} \tag{9}$$

The first-order predictive mean is calculated with Eq. (7) and mean variable dependent values.

2.2. Order of importance analysis

With the FOSM method, we are able to assess order of importance and the sensitivity influence of random input variables on output variable uncertainty [34]. The Jacobian matrix is simply a partial derivative matrix quantifying the rate of change of each input random variable with respect to the output variable. We can use the Jacobian quantification (Eq. (7)) and respective random variable standard deviations to calculate importance vectors. These importance vectors are relative measures of contribution of input variable variance to output variable variance. Knowing which input variables most greatly influence system uncertainty has major implications for control in design. We will discuss the sensitivity of random variables considered in this article in the following sections.

3. Experimental description and database

CLT full and partial penetration ballistic data are reported in [17,18] for the following species: SYP, SPF-S, thermally modified western coastal hemlock (TMWH), and western coastal hemlock (WCH). See Fig. 1 for a partial penetration plot showing DOP as a function of striking velocity. For a given target panel, [17,18] report the measured density, Janka hardness, exterior moisture content, and thickness, along with each shot in terms of projectile type, striking velocity, and resulting penetration depth or residual velocity. See Table 1 for wood species material properties, including mean, standard deviation (SD), and coefficient of variation (COV).

In this article, we add experimental results from a prominent untested structural species in the Pacific northwest, Douglas Fir (DF), and we leverage the entire CLT ballistic database in analysis.

3.1. Douglas fir CLT specimens

In the United States, three species are currently commercially manufactured into CLT: SYP, SPF-S, and DF. For ultimate integration of CLT into force protection applications, it is important to have experimental data for the true building materials candidates for broad integration. For that reason, we include results from DF specimens in the analysis. In this work, we tested two groups of DF CLT, one sourced commercially from Mercer Mass Timber in Spokane, Washington, and the other we lab fabricated at Georgia Institute of Technology's Structural Engineering

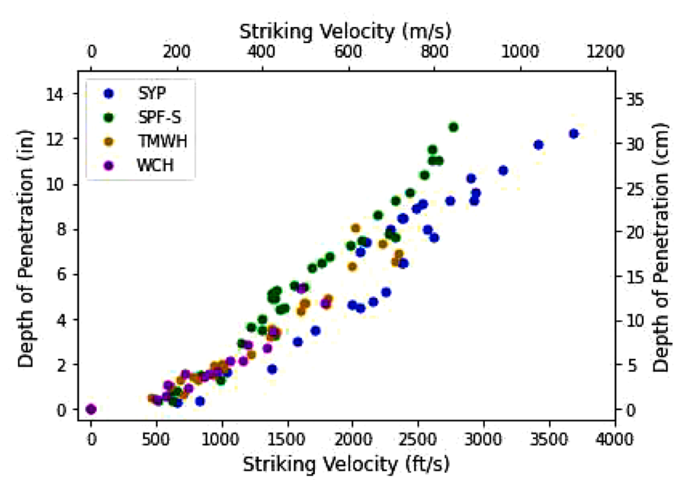

Fig. 1. Impact velocity versus depth of penetration from experimental database for SYP, SPF-S, TMWH, and WCH.

Table 1
CLT species dependent material property values.

Species	Density (lb/ft^3)			Hardness (lb)		
	Mean	SD	COV (%)	Mean	SD	COV (%)
SYP	34.9	4.26	11.9	656	196.8	30
SPF-S	27.97	2.91	9.95	605	175.45	29
TMWH	30.3	3.57	10.6	720.5	191.1	26.5
WCH	26.97	3.39	12.6	633.4	207.5	32.8

Laboratory with No 2. DF lumber, also sourced from Washington state.

For the Mercer specimens, we sourced and tested Mercer 3 and 5 ply DF CLT panels. Mercer also provided extra 2 × 6 dimensional lumber for material property experimental testing. For the lab fabricated panels, we chose to lab fabricate a series of 3 and 5 ply panels to control and label the exact board(s) of lumber used in each CLT panel. By doing this, in the case of 3 ply panels, one 8 ft (2.44 m) board of 2 × 8 lumber when cut, could make one 14 in by 14 in (35.6 cm by 35.6 cm) CLT test panel with a small amount of leftover lumber. We used the lefstover lumber for material property testing, and therefore gathered panel-specific material property distributions. This is impossible to achieve with commercially fabricated CLT due to large scale manufacturing. As a natural material with significant defects even at structural grade, measured material properties can vary greatly even within the same harvest of the same species of wood [40]. Using one board of lumber for both CLT panel fabrication and material property testing reduces uncertainty when correlating ballistic resistance of a CLT panel to quasi-static mechanical properties.

We manufactured the lab produced CLT following the guidelines and standards outlined in the CLT Handbook: U.S. Edition and Standard for Performance Rated Cross-Laminated Timber ANSI/APA PRG 320–2012 (PRG 320) [3]. Seen in Fig. 2 moving left to right, we prepared the wood for gluing by planing to 1.375 in (3.5 cm) thick, cutting 14 in (35.6 cm) long pieces, and squaring up the edges. We applied and evenly distributed on average 29 g of polyurethane adhesive within 2 h of planing to avoid dimensional instability and surface oxidation. We then stacked and set the cut pieces, alternating layer orientation ninety degrees before pressing with 100 psi of pressure for two hours. Table 2 provides the measured material properties for both groups of DF lumber, denoted Mercer DF and Lab DF with the experimental procedure used [41,42]. Referenced wood handbook values are also included [40].

3.2. *Test setup and methodology*

The ballistic experimental programs outlined in [17–19] as well as the additional experimental ballistic testing we conducted on DF CLT took place at the United States Army Corps of Engineers Engineering Research Development Center (ERDC) Fragmentation Simulating Facility (Frag Lab). The ERDC Frag Lab is an indoor climate-controlled ballistics range equipped with a smooth bore powder gun. To restrict movement during firing, the gun apparatus was bolted to the floor, and a spring system directly behind the barrel helped dissipate recoil energy. The lab has capacity for multiple smooth and rifled barrels to simulate different threats, but here, we limit the threat to a 0.50 in (1.27 cm) steel sphere projectile due to the existing CLT partial penetration database with the same projectile. For resistance against small arms, the maximum design threat defined in UFC 4–023–07 is a 50-caliber projectile. Although not a modern munition, the 0.50 in (1.27 cm) steel sphere has the same impact surface area as the maximum DOD small arms design level threat, and the results are not restricted for publication.

Moving downrange in line with the flight path of the projectile, we stationed four infrared photoelectric velocity screens connected to two chronographs to calculate the striking velocity of the projectile onto the CLT target. Two of the four velocity measurements were used to calculate striking velocity, v, with Eq. (10). Screens one and three determined v_1, and screens two and four determined v_2. The distance between screens one and three (same as two and four), L_2, was 75.625 in (192.1 cm), and the distance between screen four and the front of the CLT target, L_1, was 30 in (76.2 cm). A schematic of the experimental setup is reported in [17].

$$v = v_2 + \left(\frac{L_2}{L_1}\right)(v_2 - v_1) \tag{10}$$

Like the previous CLT ballistic experimental studies reported by [17–19], we mounted CLT targets to a rigid steel frame with rachet straps, see Fig. 3. To guarantee the same placement of specimen, we used a steel shelf attached to the frame to align each target specimen. We bolted the steel frame to a hydraulic table which locked in place during firing. The gun apparatus is in a fixed position, so to allow target panel movement (and multiple shots per panel), we slotted the hydraulic table into a ground rail to allow horizontal movement in addition to the built-in vertical positioning ability.

[18] showed with nondestructive post-mortem computed tomography (CT) imaging the highly localized fracture interaction zone in the CLT resulting from a partial ballistic penetration. This highly localized damage radius allowed multiple shots per panel assuming no interaction between shots. All panels except two DF Lab panels were shot five times, with one shot in the center and one in each corner, 2 inches (5.1 cm) from each edge. The two DF lab panels were shot 8 and 9 times, respectively, for a repeat velocity experiment. Post testing, the DF lab panels were cut open to again insure no visible interaction between shot paths.

Typically, we use high speed phantom cameras to capture exit velocities, but here we only conducted partial penetration experiments. We measured depth of penetration by prodding a thin metal rod through the depth of each specimen shot path until we contacted the front of the spherical projectile. We measured the metal rod depth with calipers, and added the diameter of the projectile, 0.5 in (1.27 cm) to measure penetration depth.

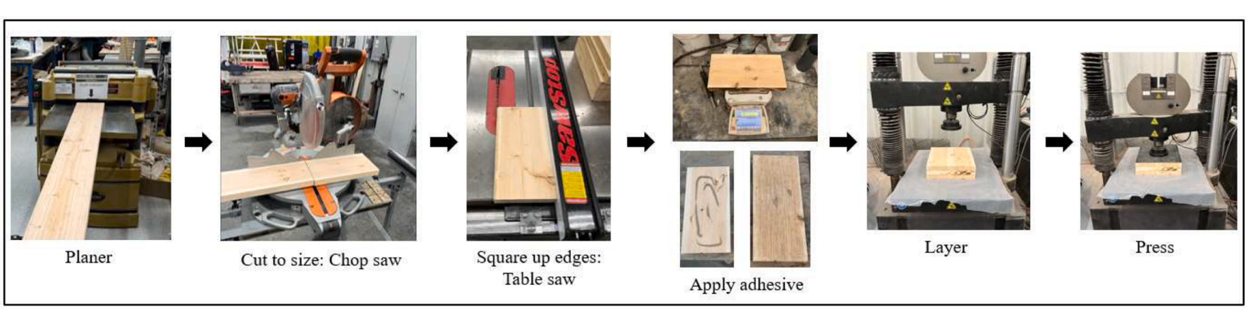

Fig. 2. Lab scale CLT manufacturing procedure.

Table 2
Lab and Mercer DF material property values.

Material Property	Method	Direction	Mercer DF Mean	Mercer DF SD	Mercer DF COV (%)	Mercer DF N	Lab DF Mean	Lab DF SD	Lab DF COV (%)	Lab DF N	Reference Wood Handbook values Mean
Density, lb/ft^3	ASTM D2395	N/A	34.0	3.01	8.86	30	30.3	3.84	12.7	69	29.95
Janka Hardness, lb	ASTM D143	Tangential	734.4	180.0	24.5	18	581	180	31.1	46	710
		Radial	696.8	91.5	13.1	12	597	119	20	22	–
		Longitudinal	783.0	153.6	19.6	10	798	148	18.5	11	–
Compressive strength (psi)	ASTM D143	Tangential	817.1	59.1	7.24	8	702.6	220.8	31.4	13	800
		Radial	967.2	30.3	3.13	8	810.0	341.7	42.2	14	–
		Longitudinal	7376	1043	14.1	12	5938	768.5	12.9	6	7230
Compressive modulus (psi)	ASTM D143	Tangential	18,185	1361	7.48	8	20,177	6729.8	33.4	13	–
		Radial	63,411	5992	9.45	8	24,300	10,150	41.8	14	–
		Longitudinal	815,694	181,437	22·2	12	719,390	64,412	8.95	6	–
Modulus of rupture (psi)	ASTM D143	N/A (tangential)	20,840	1846	8.86	8	12,704	3417	26.9	6	12,400
Modulus of elasticity (psi)	ASTM D143	N/A	2.45×10^6	1.83×10^5	7.48	8	1.46×10^6	2.47×10^5	16.9	6	1.95×10^6
Work to maximum load (lb-in)	ASTM D143	N/A	395.5	86.2	21.8	8	151.5	89.7	59.2	6	138.6

Fig. 3. CLT target specimen and fixture.

4. Experimental results

In this section, we will report the DF ballistic experimental results (and integration into the global CLT ballistic database). Leveraging the CLT partial penetration database, we will update a global UFC equation from Eqs. (1) and Eq. (6) for utilization in FOSM predictive analysis.

4.1. Douglas fir experimental results

We conducted 61 total partial penetration shots with a 0.50 in (1.27 cm) steel sphere projectile, 29 on the Mercer DF and 32 on the Lab DF, see Fig. 4(a). Like the partial penetration profiles developed by [17,18] seen in Fig. 1., we can use these experimental profiles to determine the ballistic resistance of a CLT target to a certain threat, and fit design curves. In addition to building partial penetration curves, we conducted a series of shots at the same target striking velocity to investigate ballistic variability holding target striking velocity constant, see Fig. 4(b). For the Mercer DF CLT, we shot two panels for a total of ten shots at 1700 ft/s (518.2 m/s) target striking velocity. For the lab DF CLT, we shot two panels for a total of 17 shots at 1200 ft/s (365.8 m/s) target striking velocity. We were able to use this partial penetration data when evaluating the validity and sensitivity of the FOSM predictive results. We added the DF partial penetration datasets to the existing CLT database.

4.1.1. Output random variable distribution

To evaluate normality of the output random variable such that FOSM can be reliably used, we assessed the distributions of measured DOP values. Because we conducted repeat target striking velocity

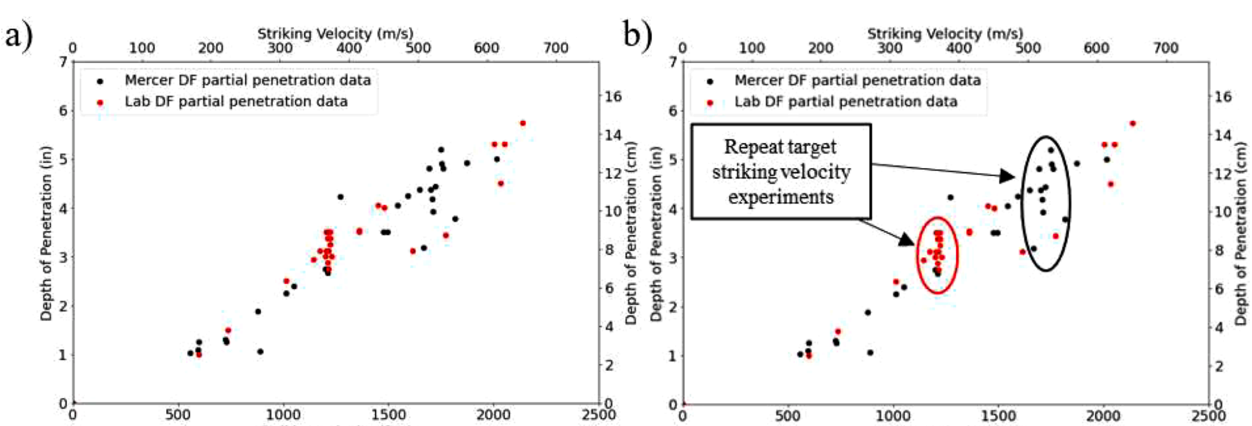

Fig. 4. a) Impact velocity versus depth of penetration for lab and commercially fabricated DF CLT b) Repeat target striking velocity experiments.

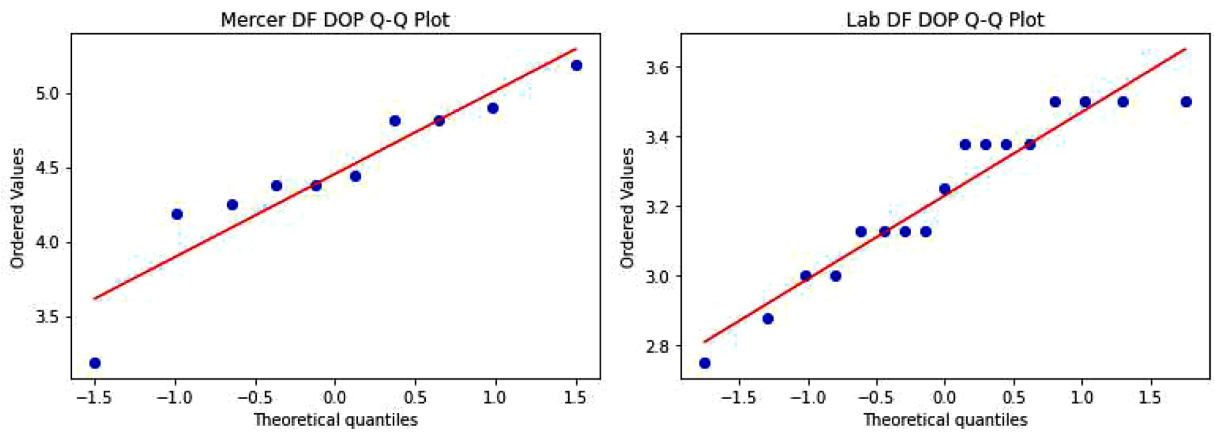

Fig. 5. Q-Q plots to assess DOP normality.

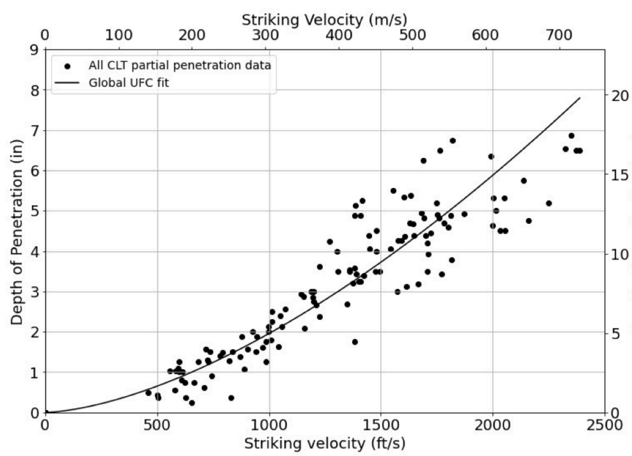

Fig. 6. Global UFC equation (Eq. (11)) fit to all known CLT 0.50-caliber steel sphere projectile data.

experiments on both the Mercer and Lab DF CLT, we could assess if the resulting DOP data distributions are normal, and therefore appropriate candidates for the FOSM method. We used the null hypothesis Shapiro-Wilk Test to assess normality of both DOP distributions, and the quantile-quantile plot for visual assessment, see Fig. 5. The p-value for the Mercer DF was 0.180, and 0.103 for the Lab DF, showing normality with a p-value greater than 0.05 for both datasets. The data follows the theoretical 45-degree normal distribution line which alone does not confirm normality, but acts as a visual check in combination with the Shapiro-Wilk Test. The outcomes indicate appropriateness of the FOSM predictive method for our dataset.

4.2. Global UFC update

In UFC 4–023–07, a single equation is presented to design a wood structure against any small arms threat for listed wood species, with density and hardness values tabulated in the standard [18] assessed the validity of using one form of the UFC equation for (at the time) all CLT ballistic data by recalibrating fitting coefficients with least squares regression [18] showed that while mean squared error and correlation coefficient for each dataset were higher than respective individual fits, the difference was small, with mean squared error differing at a maximum of 1.438 in^2, and difference in correlation coefficient of 0.048. This has major implications for design criteria moving forward as fitting separate models to individual species requires significant, unlikely to be obtained data. If a single global equation can be found, we can leverage previous foundational data to fit and predict new species resistances. With this in mind, we again fit a single UFC equation to all available partial penetration data, see Eq. (11), which we then utilize throughout all FOSM predictive calculations. A graphical representation of the global UFC equation curve is seen in Fig. 6. where the experimental data is represented by points and the UFC a continuous curve. To plot the UFC curve, we utilized average density and hardness values across all CLT datasets without separating out by species. The global UFC equation fits the data well with mean squared error equaling 0.351 in^2. We can also see that scatter in DOP increases as striking velocity increases.

$$DOP_{Global} = 0.681\left(\frac{v^{1.588}w^{1.056}}{\rho\left(\frac{\pi D^2}{4}\right)^{0.610} H^{0.5}}\right) \quad (11)$$

5. FOSM approximation and prediction results

In this section we assess the accuracy and robustness of using the FOSM method to predict DOP mean and variance values across different data groupings or sorting categories. In structural wood design, separating design values such as bending or shear strength by species and lumber grade is the standard [43]. We will first follow convention, but we also have the opportunity to define material input distributions for any data subgroup. For example, we can input average and standard deviation material property values as broad as the entire CLT database but also as specific as a single panel, and estimate results. For this predictive method to be used with confidence, validating results against different groupings of data is necessary, as shown in the following subsections.

5.1. Mercer DF

We first apply the FOSM method to the Mercer DF CLT subgrouping, and more specifically at one target striking velocity. We sampled five lumber boards supplied by Mercer, taking three hardness measurements in both the tangential and radial directions from each board. Before hardness testing, we measured density to allow quantification of correlation between material properties. The correlation between density and hardness was $R_{\rho H} = 0.56$. For ballistic testing, we conducted ten repeat shots at 1700 ft/s (518.2 m/s) target striking velocity, see Fig. 4a for a raw striking velocity vs. DOP plot. It is important to note there is variability in the experimental striking velocity itself. In powder-based ballistic experimentation, it is difficult to successfully repeat shots at the exact same target striking velocity. This variability, although not typically accounted for, can be integrated into the random variable descriptions utilized in the FOSM approximation, providing a more complete representation of the uncertainties present in the projectile-target system. See Table 3 for random variable means and coefficients

Table 3
Random variable means and COVs.

Random variable	Mean	COV
Striking Velocity (ft/s)	1698	0.0292
Density (lb/ft^3)	34.00	0.0886
Hardness (lbs)	719.4	0.2110
Projectile Weight (lbs)	0.0183	0.0020
Projectile Diameter (in)	0.5000	0.0020

of variation (COVs).

Utilizing the global UFC equation defined in Eq. (11) and the FOSM method outlined in Section 2, we calculated predictive compared to true experimental values, with results shown in Table 4. We ran iterations of the FOSM estimate assuming both true correlation and no correlation (independence) between random variables for comparison. We calculated experimental and predictive COVs to compare uncertainty in the predictions with those from the actual experimental results.

With these results, we can numerically compare the experimental and predictive values, but it is difficult to assess adequacy of the prediction based on numerical mean and standard deviation comparisons alone. For example, from Table 4, we see that the mean DOP is slightly underpredicted, leading to potentially unconservative designs. At the same time, the standard deviation and coefficient of variation are overpredicted, suggesting conservative predictive results. These observations appear to contradict each other. The case assuming independence between random variables decreases uncertainty, therefore decreasing the predicted standard deviation prediction, aligning closer to the experimental value. To better evaluate the accuracy of the prediction for use in force protection design, we assess the results statistically. Fig. 7 shows the raw data, mean estimations as solid curves (with the experimental values in black and the UFC global fit in grey), and 95 % confidence intervals based on the experimental (darker grey) compared to predicted (lighter grey) data. Looking at the mean estimations, we see that just using the global UFC fit equation underpredicts the DOP, and using the 95 % confidence interval calculated from just the experimental data covers the measured data. However, looking at the predictive confidence interval, we see that the 95 % confidence interval predictive bounds generated by the UFC global curve and the FOSM method to assess uncertainty in CLT resistance fully covers all measured experimental data.

5.1.1. Order of importance

The results of the order of importance analysis are shown in Table 5 for the five input random variables defined in Eq. (11). For the Mercer DF experiment, hardness and density are the most important random variables followed by striking velocity. It is important to note that the results shown in this section are based on DOPs measured at the same target striking velocity. Therefore, the importance of striking velocity is lower here than for a full partial penetration profile, which is a strong function of striking velocity. The importance vector shown in Table 5 tells us that the material-level variability of wood has the largest influence on the resulting uncertainty of ballistic resistance.

5.1.2. Extension to full partial penetration profile

We now extend the analysis to the entire Mercer DF partial penetration profile. Fig. 8 shows the raw Mercer DF partial penetration data across striking velocities, the UFC global fit with Mercer DF average density and hardness values found in Table 2, and the experimental and

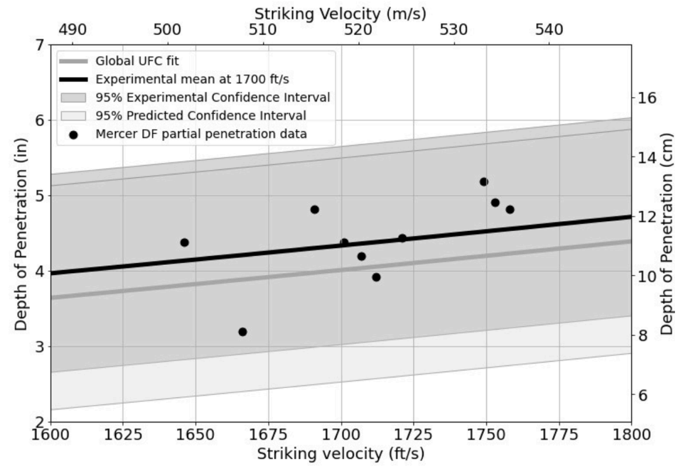

Fig. 7. Mean and 95 % confidence interval predictive bounds for impact velocity vs depth of penetration for Mercer DF repeat experiments.

Table 5
Order of importance.

v	ρ	H	w	D
0.034	0.125	0.177	7.08×10^{-5}	9.445×10^{-5}

predicted 95 % confidence intervals based on the calculated values shown in Table 6. We see the UFC global equation alone overpredicts resistance, but by adding variance approximations through the FOSM method and therefore predicting resistance as a distribution, we are able to truly capture the inherent variability tied to CLT and all wood materials. One DOP datapoint (collected at 1270 ft/s (387 m/s)) fell outside both experimental and predicted 95 % confidence intervals. This shot directly impacted the seam between two adjacent wood laminas, offering less target resistance. Utilizing standardized residuals outlier criteria with a threshold of 2, this datapoint was deemed an outlier, and is represented as an x in Fig. 8.

We can extend the order of importance analysis across striking velocities, see Table 6. The importance vectors increase proportionally as striking velocity increases, showing material-level variability has the largest influence on the resulting uncertainty of ballistic resistance for an entire partial penetration profile.

5.2. Lab DF

Our lab-fabricated DF panels enabled us to capture panel-specific material properties, including means and standard deviations of panel-specific density and hardness as shown in Table 7. To evaluate the sensitivity of the FOSM approximation, we calculate a series of estimations utilizing panel-specific material and ballistic data. We conducted repeat ballistic experiments on two panels, DF1 and DF6, at 1200 ft/s (365.8 m/s) target striking velocity. With the FOSM method, we can predict not only the means and standard deviations of the individual panels, but also their combination. It is important to note the significant difference in correlation between density and hardness in DF1 and DF6. This could be due to a multitude of factors but is likely caused by defect distributions in the wood we sampled. As a natural material, wood is

Table 4
Mercer DF CLT FOSM results in predicting DOP.

Species	Experimental				Predictive		
DF- Mercer	μ (in)	σ (in)	COV (%)		μ (in)	σ (in)	COV (%)
	4.310	0.522	12.1	$R_{\rho H} = 0.56$	3.985	0.709	17.8
				$R_{\rho H} = 0$		0.579	14.5

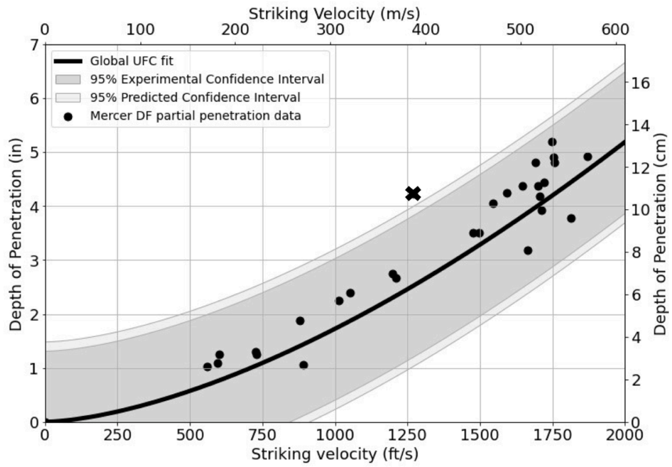

Fig. 8. Mean and 95 % confidence interval predictive bounds for impact velocity vs depth of penetration for Mercer DF partial penetration profile.

prone to defects such as checking or voids at the macro and micro scale. Density is a bulk quantity while hardness is highly localized, so any defects or imperfections in the surface area utilized for indentation testing to obtain hardness values could drastically decrease localized strength [40]. Here we have two lumber boards of the same source, species, and grade with different densities, hardnesses, and correlations between the two. These panels are nearly as experimentally selective and controlled as feasible, so we are truly highlighting the large inherent variability of wood and the need to explicitly consider uncertainty and design for this variability.

Like the Mercer DF CLT, we can directly compare the FOSM predictions to experimental results. See Table 8 for experimental and predictive means, standard deviations, and COVs, all at 1200 ft/s (365.8 m/s) target striking velocity. Again, we ran predictions with both the true correlation between density and hardness, as well as independence between all random variables. For visualization and comparison, Fig. 9 shows the raw data, mean estimations as solid curves (with the experimental values in the darker color and the UFC global fit in the lighter color), and 95 % confidence intervals based on the experimental (darker grey) compared to predicted (lighter grey) data for individual panel DOP distributions and their combination. From Table 8, we see the FOSM slightly underpredicts the mean DOP, and overpredicts the standard deviation. Although the mean DOP is slightly underestimated, predictive 95 % confidence bounds fully capture each experimental dataset, serving as adequate predictions. Looking at the individual panels and their combination, we see that although the predictive values do not match perfectly, the experimental and predictive trends do, i.e., the DF6 mean DOP is greater than the combination of DF1 and DF6, and is further greater than the DF1 DOP mean. The FOSM predicted this trend for both mean and standard deviation. Here we were able to define panel-specific material property random variables, variations, and correlations for a FOSM approximation. All predictions provide full coverage of the data within 95 % confidence bounds, showing the adequacy of the method when random variables are completely defined, even with a small dataset.

5.3. Extension to CLT species dependent datasets

Now, we extend this predictive method to our six species dependent groups of ballistic partial penetration data. Unlike the Mercer and Lab DF datasets, we often do not have a series of datapoints at repeat target striking velocities due to limited target material and prioritization of building out partial penetration curves by gradually stepping target striking velocity, as is typical for historically used protective materials. Also, although we do have density and hardness data for all species tested, we do not universally have recorded panel-specific properties, nor do we know exact correlations between the two wood material properties. The Mercer DF material testing served as highly controlled commercially fabricated primary data, so as an initial approximation, we assumed all species had a positive correlation between hardness and density, mimicking the DF Mercer wood. We showed the wide range of density and hardness correlations in the Lab DF lumber, and selected a

Table 6
Order of importance across striking velocities.

Striking velocity (ft/s)	v	ρ	H	w	D
0	0	0	0	0	0
500	7.02×10^{-4}	0.003	0.004	1.455×10^{-6}	1.941×10^{-6}
1000	0.006	0.023	0.033	1.316×10^{-5}	1.755×10^{-5}
1500	0.023	0.084	0.119	4.770×10^{-5}	6.360×10^{-5}
2000	0.057	0.210	0.297	1.190×10^{-4}	1.587×10^{-4}

Table 7
Lab DF material property values.

Panel	Density			Hardness			
	μ (in)	σ (in)	COV (%)	μ (in)	σ (in)	COV (%)	$R_{\rho H}$
DF1	29.7	1.60	5.4	550.4	118.6	21.5	0.249
DF6	28.7	0.899	3.14	557.0	49.1	8.81	0.880
Combination	29.3	1.43	4.86	553.1	94.4	17.1	0.292

Table 8
Lab DF FOSM results in predicting DOP.

Panel ID	Experimental			Prediction			
DF1	μ (in)	σ (in)	COV (%)		μ (in)	σ (in)	COV (%)
	3.089	0.236	7.64	$R_{\rho H} = 0.249$	3.053	0.404	13.2
				$R_{\rho H} = 0$		0.369	12.1
DF6	3.325	0.188	5.65	$R_{\rho H} = 0.88$	3.134	0.238	7.16
				$R_{\rho H} = 0$		0.181	5.44
Combination	3.23	0.235	7.27	$R_{\rho H} = 0.292$	3.083	0.343	11.1
				$R_{\rho H} = 0$		0.308	10.0

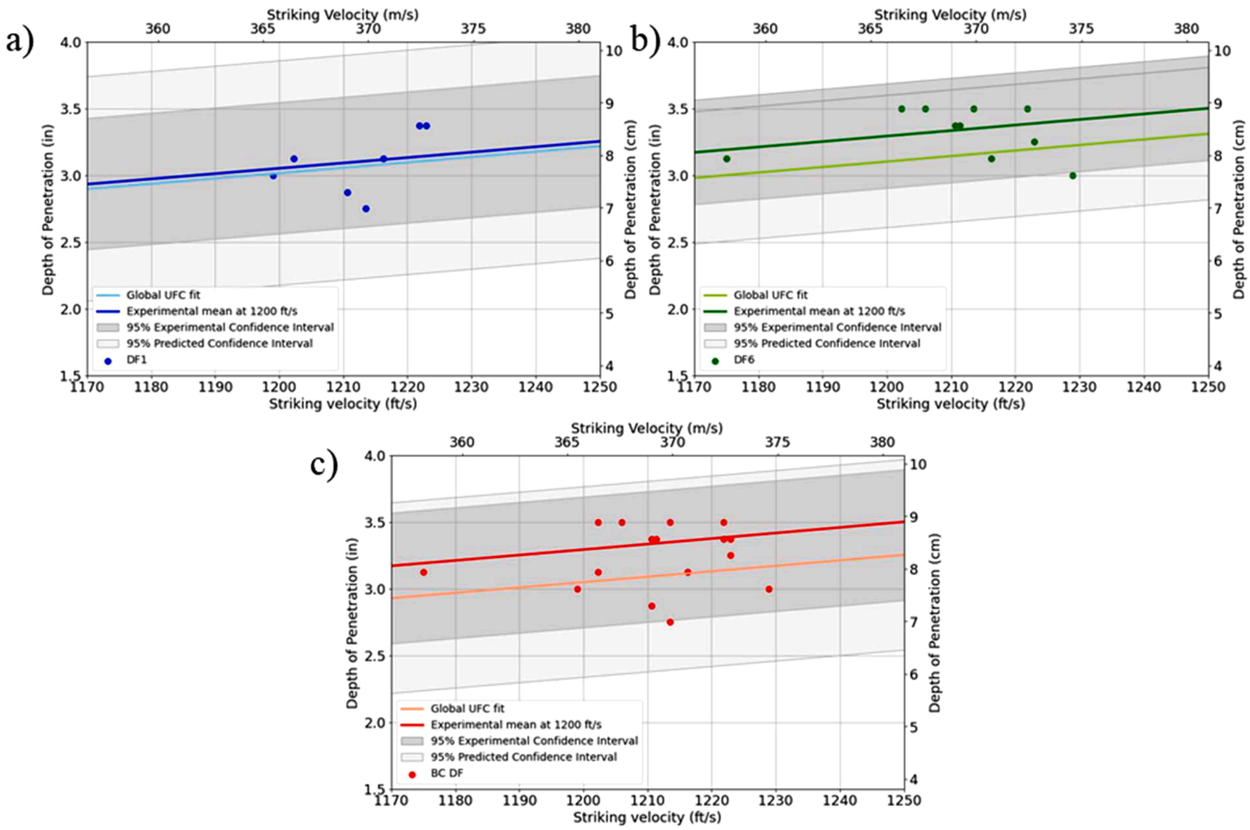

Fig. 9. a) Experimental data and results for individual DF1 CLT panel (b) Experimental data and results for individual DF6 CLT panel (c) Experimental data and results for combined DF CLT two panel dataset.

Table 9
Species dependent FOSM predictions.

Species	FOSM Prediction			
DF- Mercer	$R_{\rho H}$	μ (in)	σ (in)	COV (%)
	0.56	3.985	0.709	17.8
	0		0.579	14.5
DF- Lab	0.56	4.942	1.188	24.0
	0		0.962	19.5
SPF-S	0.56	5.296	1.175	22.2
	0		0.963	18.2
SYP	0.56	4.066	0.986	24.2
	0		0.801	19.7
WCH	0.56	5.354	1.309	24.4
	0		1.075	20.1
TMWH	0.56	6.372	0.871	13.7
	0		0.709	11.1

middle ground $R = 0.56$ as an appropriate assumption for the other species datasets. In practice, we know the uncertainty of the FOSM DOP estimation increases with increased correlation between density and hardness, so if not explicitly known, choosing a higher correlation value is conservative.

Similar to the analysis shown in Fig. 8, except now for the full CLT dataset, we fit the UFC global equation to each species subset using species-specific material input parameters. We predicted variance of each species subset using the FOSM method, and tabulated results in Table 9 for both 0.56 material level correlation and assuming independence between all variables. Results are plotted in Fig. 10 for the five wood species. Here we are not able to directly compare estimations to repeat velocity data like with the Mercer or Lab DF CLT, so comparing complete bounds to experimental profiles (and subsequent confidence intervals) is crucial to assess if predictions are valid.

For each species dependent partial penetration profile, the FOSM estimation fully captured each experimental 95 % partial penetration confidence interval and all experimental datapoints. To emphasize the impact and implications of this analysis, we are using a method that utilizes a closed form global predictive equation with two surface-level easy-to-attain wood material inputs and projectile parameters to accurately and robustly predict ballistic resistance performance. The FOSM method is a straightforward and fast computational tool that uses material-level property variability to predict global ballistic resistance within 95 % confidence for different species subsets. This can be compared to numerical models that are certainly important to investigate material performance, but, for example, require nine elastic constants (elastic modulus, Poisson's ratio, and shear modulus in three principal directions) to just build an elastic stiffness matrix for orthotropic materials such as wood. In the above analysis, we showed we can characterize an extremely complicated material under a dynamic localized loading condition with an appropriately applied simple reliability-based predictive method.

Thinking about design in a force protection environment, we can use the FOSM distribution prediction as the baseline for safety factor application. Because we can predict holistic penetration resistance with confidence, informed safety factors can be determined depending on a number of application-specific factors. Without a baseline resistance profile as made possible by this work, blind, likely overconservative safety factors would be used, and the design thickness of CLT needed for protection would be unrealistic for field applications, limiting the use of the material. We have advanced the predictive understanding of CLT ballistic resistance to allow educated and safe use of the building material in domestic and international force protection applications.

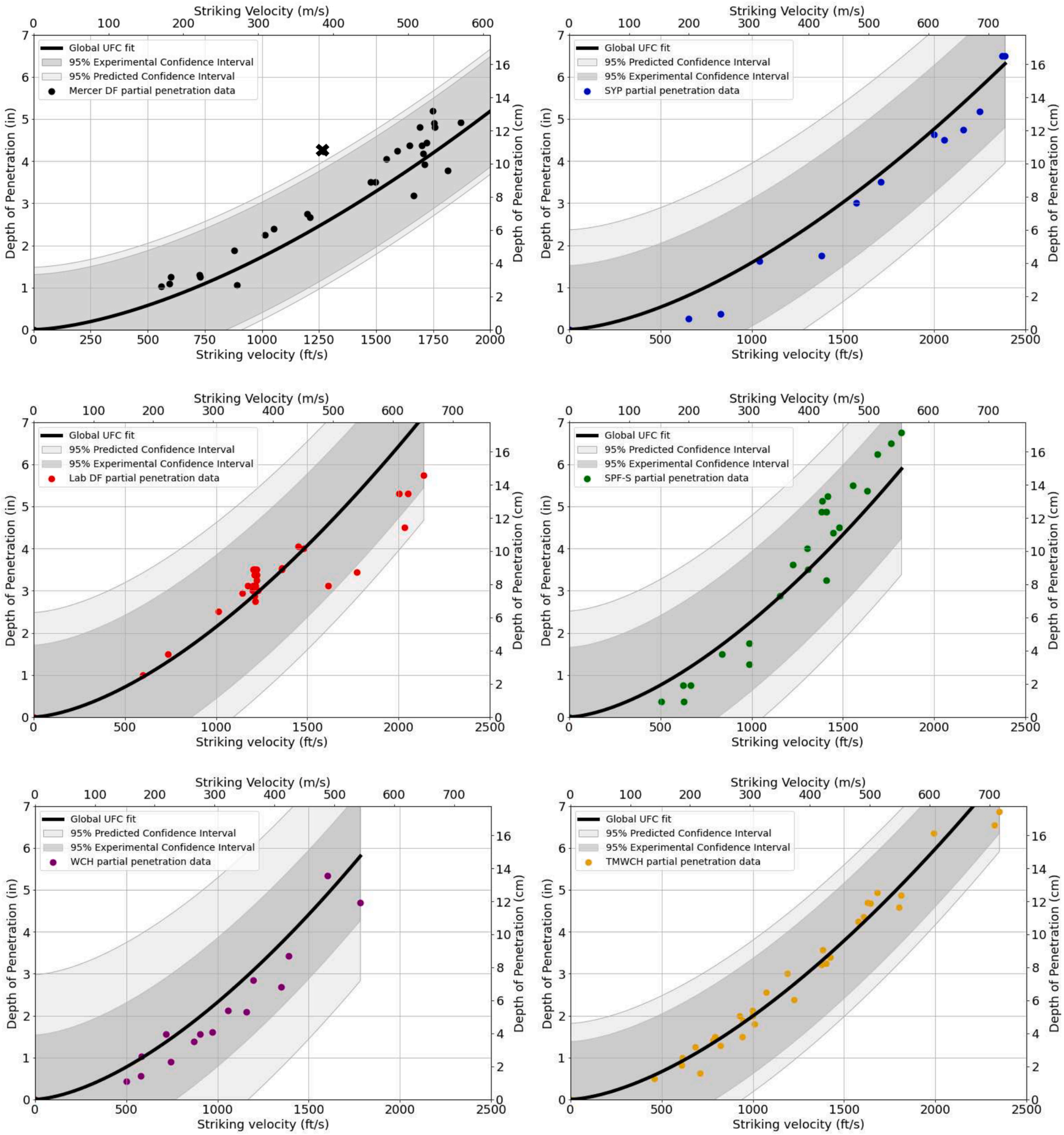

Fig. 10. Species dependent partial penetration profiles, global UFC fit mean, and experimental compared to predictive FOSM 95 % confidence interval bounds.

5.4. Predicting CLT resistance based on density

From the order of importance analysis in Section 5.1.1, we found that uncertainty in wood material most greatly influences uncertainty in resulting ballistic resistance when subjected to the same loading. With this finding, we hypothesized that sorting CLT ballistic data by density rather than species would reduce resistance uncertainty along a partial penetration profile. With the panel-specific density data available, we sorted ballistic partial penetration data by density to the nearest whole integer, differentiating by a color gradient moving from low to high density with dark to light, see Fig. 11(a). There is a clear separation as the density jumps from 30 lb/ft^3 to 34 lb/ft^3, so we grouped the data by "low" (27–30 lb/ft^3) and "high" (34–40 lb/ft^3) density profiles, see Fig. 11(b). This range of densities are typical for any softwood species, and are likely to fluctuate within the same board of wood due to natural moisture changes. We plotted the global UFC equation with the low and high density profiles, again inputting average density and hardness material values, see Fig. 11(c). The predictive UFC profiles fit each density dataset with low error, and the scatter around each curve is minimal, even still using ranges of densities and hardnesses. The predictive 95 % confidence intervals are narrower compared to species dependent dataset predictions, showing reduced uncertainty when sorting by density.

The impact here is twofold. First, we have showed that if the density of CLT panels is controlled and variability is minimized, ballistic resistance uncertainty is minimized. Density is measured nondestructively, meaning we can know the exact densities of wood boards used for CLT manufacturing, and therefore we can produce panels to certain force protection uncertainty tolerances. Second, if ballistic profiles can be predicted based on wood density, softwood multi-species CLT systems

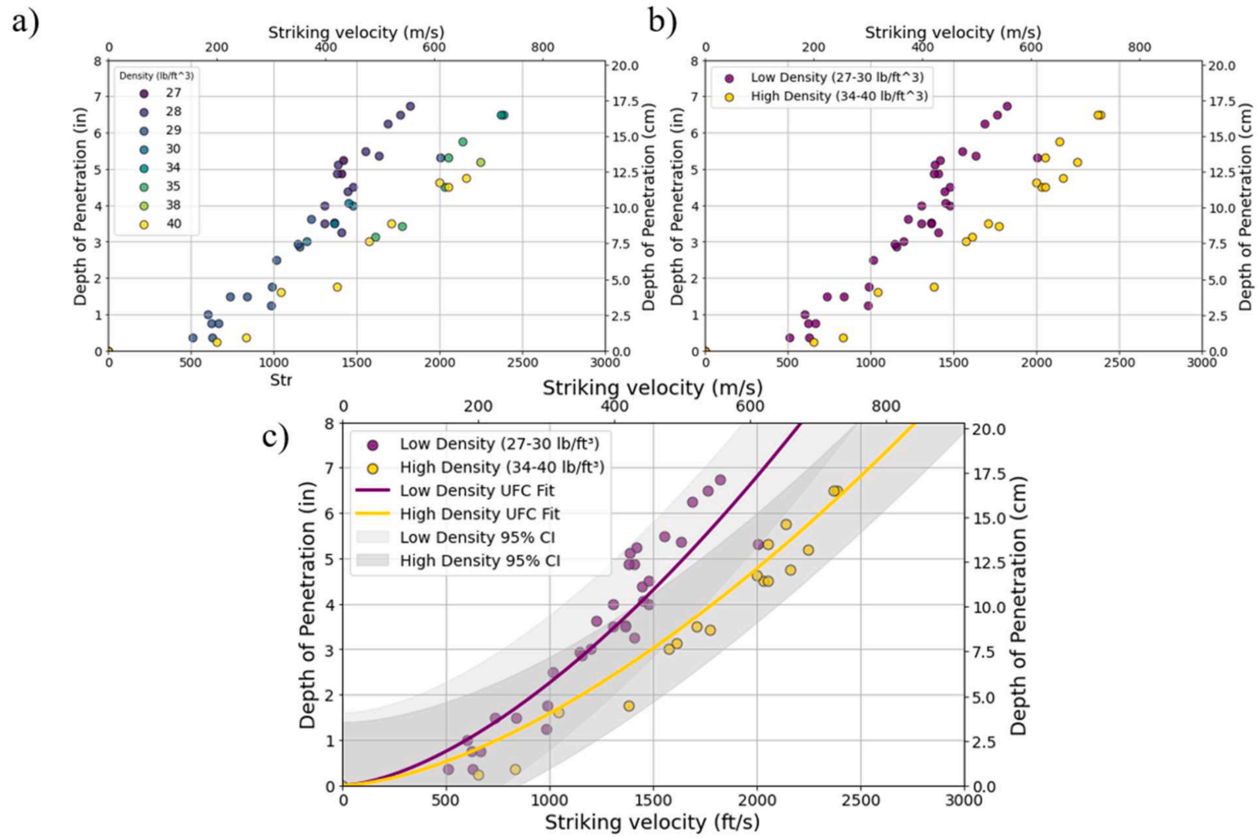

Fig. 11. a) Impact velocity vs. depth of penetration for CLT sorted by panel density to the nearest whole integer b) Separation into low and high density groups c) Global UFC fit and predictive 95 % confidence intervals to low and high density partial penetration profiles.

could be used if density is controlled. Thinking about a deployed environment where building materials typically need to be locally sourced, we often will not know exact tree species, but we can easily measure density to estimate ballistic resistance. This conclusion furthers the use case of CLT and wood products in force protection environments, and the methodology described in this study provides a straightforward, accurate, and robust way to predict ballistic resilience for these materials.

6. Conclusions

(1) We added an untested prominent structural species in the Pacific Northwest, Douglas Fir, to the CLT ballistic database. In addition to building partial penetration profiles, we investigated variability at the material property level and response variability under ballistic impact for both commercially manufactured and lab produced Douglas Fir CLT.

(2) We defined a single global CLT UFC partial penetration equation leveraging six unique CLT species-specific ballistic datasets, including the three species currently used in commercial CLT manufacturing; Southern Yellow Pine, Spruce Pine Fir – South, and Douglas Fir.

(3) With the CLT UFC formulation, we applied the first-order second-moment method to estimate partial penetration means and standard deviations. We used this simple reliability-based method to characterize and capture the inherent variability of CLT under ballistic impact, and represent resistance profiles as distributions rather than single values. We applied the predictive method at different scales, from Douglas Fir panel-specific single velocity estimates to full species partial penetration profiles. For each data grouping, the FOSM prediction captured within 95 % confidence intervals the experimental dataset.

(4) We argue the FOSM predictions should act as a baseline resistance curve for CLT ballistic design. With full characterization of CLT ballistic profiles and inherent scatter, informed safety factors can be applied by situational decision makers in permanent or deployed environments.

(5) Wood material variability (density, hardness, and their correlation) are the most important contributions to ballistic resistance uncertainty under the same loading. When sorting ballistic partial penetration data by density instead of species, we observed clear separation and reduced scatter in partial penetration profiles, sorting by 27–30 lb/ft^3 and 34–40 lb/ft^3 data groupings. Controlling density variability in a CLT system will reduce ballistic resistance variability, and could allow for multi-species system utilization.

(6) This article shows the power of using an established computationally inexpensive reliability- based predictive method to characterize a dynamic complex engineering problem. We adequately predicted all CLT partial penetration profiles and distributions with simply two wood material properties, striking velocity, and projectile parameters.

CRediT authorship contribution statement

Juliet Swinea: Writing – review & editing, Writing – original draft, Visualization, Validation, Methodology, Investigation, Formal analysis, Data curation, Conceptualization. **Iris Tien:** Writing – review & editing, Visualization, Validation, Supervision, Methodology, Investigation, Formal analysis, Conceptualization. **Peter Stynoski:** Writing – review & editing, Validation, Project administration, Methodology, Funding acquisition, Conceptualization. **Lauren K. Stewart:** Writing – review & editing, Validation, Supervision, Resources, Project administration, Methodology, Conceptualization.

Declaration of competing interest

The authors declare that they have no known competing financial interests or personal relationships that could have appeared to influence the work reported in this paper.

Acknowledgements

This material is based upon work supported by the US Army Engineer Research and Development Center (ERDC) through a mentor/mentee relationship created by the Science, Mathematics, and Research for Transformation (SMART) Scholarship for Service program. The tests described and the resulting data presented herein, unless otherwise noted, are supported under PE 0603119A, Project BO3 'Military Engineering Technology Demonstration (CA)', Task 'Program Increase - Cross-Laminated Timber'. properties, striking velocity, and projectile parameters.

Data availability

Some or all data, models, or code that support the findings of this study are available from the corresponding author upon reasonable request.

References

[1] Karacabeyli E, editor. CLT handbook: cross-laminated timber. U.S. edition. Pointe-Claire, QC: FPInnovations; 2013.
[2] Mohammad M, Gagnon S, Douglas B, Podesto L. Introduction to cross laminated timber. Wood Des Foc 2012;22.
[3] Standard for performance-rated cross-laminated timber. APA – The Engineered Wood Association; 2018.
[4] Abed J, Rayburg S, Rodwell J, Neave M. A review of the performance and benefits of mass timber as an alternative to concrete and steel for improving the sustainability of structures. Sustainability 2022;14(9):5570. https://doi.org/10.3390/su14095570.
[5] Ayanleye S, Udele K, Nasir V, Zhang X, Militz H. Durability and protection of mass timber structures: a review. J Build Eng 2022;46:103731. https://doi.org/10.1016/j.jobe.2021.103731.
[6] Ghobadi M, Sepasgozar SME. Circular economy strategies in modern timber construction as a potential response to climate change. J Build Eng Oct. 2023;77:107229. https://doi.org/10.1016/j.jobe.2023.107229.
[7] Heymsfield E, Rueppel T, Stynoski P. State-of-the-art review of Mass timber design standards and specifications. J Arch Eng 2024;30(4):03124006. https://doi.org/10.1061/JAEIED.AEENG-1802.
[8] Bhandari S, Riggio M, Jahedi S, Fischer EC, Muszynski L, Luo Z. A review of modular cross laminated timber construction: implications for temporary housing in seismic areas. J Build Eng 2023;63:105485. https://doi.org/10.1016/j.jobe.2022.105485.
[9] Sanborn K. Exploring cross-laminated timber use for temporary military structures: ballistic considerations. Georgia Institute of Technology; 2018.
[10] M. Weaver, M. Lo Ricco, A. Senalik, J. Cattelino, R. Tudhope, and P.W. van der Meulen, "Development of a cost-effective CLT panel capable of resisting DOS/DOD Deisgn basis threats," Karagozian & Case, Final Accomplishment Report TR-19-41.2, Oct. 2020.
[11] "Analysis guidance for cross-laminated timber construction exposed to airrblast loading," PDC-TR 18-02, Sept. 2018.
[12] Flores NR, Gentry R, Stewart LK. Behavior and damage characterization of impulsively loaded cross-laminated timber panels. Appl Sci 2022;12(23):12076. https://doi.org/10.3390/app122312076.
[13] Lopez-Molina A, Doudak G. Retrofit techniques for Cross-laminated timber (CLT) elements subjected to blast loads. Eng Struct 2019;197:109450. https://doi.org/10.1016/j.engstruct.2019.109450.
[14] Lowak MJ. Static and dynamic testing of cross-laminated timber panels. Bak Eng Risk Consult Feb. 2016.
[15] Poulin M, Viau C, Lacroix DN, Doudak G. Experimental and analytical investigation of cross-laminated timber panels subjected to out-of-plane blast loads. J Struct Eng 2018;144(2):04017197. https://doi.org/10.1061/(ASCE)ST.1943-541X.0001915.
[16] Sanborn K, Riser B, Gentry R, Stewart L. Ballistic performance of enhanced cross-laminated timber (ECLT). presented at the SUSI 2018 June 2018:267–78. https://doi.org/10.2495/SUSI180241.
[17] Sanborn K, Gentry TR, Koch Z, Valkenburg A, Conley C, Stewart LK. Ballistic performance of Cross-laminated Timber (CLT). Int J Impact Eng 2019;128:11–23. https://doi.org/10.1016/j.ijimpeng.2018.11.007.
[18] Swinea J, Stynoski P, Lessel A, Wood G, Stewart LK. Effect of thermal modification on the ballistic performance of coastal western hemlock Cross-laminated timber (CLT). Int J Impact Eng 2023;182:104769. https://doi.org/10.1016/j.ijimpeng.2023.104769.
[19] Swinea J, Sanborn K, Weaver M, Ricco ML, Senalik CA, Stewart LK. Enhanced cross laminated timber (ECLT) for ballistic resistant design. Int J Impact Eng 2024;189:104931. https://doi.org/10.1016/j.ijimpeng.2024.104931.
[20] Viau C, Doudak G. Behaviour and modelling of cross-laminated timber panels with boundary connections subjected to blast loads. Eng Struct 2019;197:109404. https://doi.org/10.1016/j.engstruct.2019.109404.
[21] Gilbertson CG, Bulleit WM. Load duration effects in wood at high strain rates. J Mater Civ Eng 2013;25(11):1647–54. https://doi.org/10.1061/(ASCE)MT.1943-5533.0000708.
[22] M. Weaver, C. Newberry, C. O'Laughlin, and L. Podesto, "Results from blast tests of full-scale cross-laminated timber structures," Karagozian & Case, TR-17-17.1, Sept. 2017.
[23] Unified facilities criteria design to resist direct fire weapons effects (UFC 4-023-07). U.S. Department of Defense; Feb. 01, 2017.
[24] Foschi RO. Reliability applications in wood design. Prog Struct Engng Mater Apr. 2000;2(2):238–46. https://doi.org/10.1002/1528-2716(200004/06)2:2%3C238::AID-PSE29%3E3.0.CO;2-X.
[25] The chemistry of Solid wood. In: Rowell R, editor. Advances in chemistry, vol. 207. Advances in chemistry, vol. 207, 207. Washington, DC: American Chemical Society; 1984. https://doi.org/10.1021/ba-1984-0207.
[26] Radkau J, Camiller P. Wood: a history. Cambridge: Polity press; 2012.
[27] Hetherington JG, Rajagopalan BP. An investigation into the energy absorbed during ballistic perforation of composite armours. Int J Impact Eng Jan. 1991;11(1):33–40. https://doi.org/10.1016/0734-743X(91)90029-F.
[28] Iqbal MA, Senthil K, Bhargava P, Gupta NK. The characterization and ballistic evaluation of mild steel. Int J Impact Eng 2015;78:98–113. https://doi.org/10.1016/j.ijimpeng.2014.12.006.
[29] Koene L, Broekhuis FR. Bullet penetration into wooden targets. In: 30th International Symposium on Ballistics. DEStech Publications, Inc.; 2017. https://doi.org/10.12783/ballistics2017/16976.
[30] Ellingwood BR. Probability-based LRFD for engineered wood construction. Struct Saf 1997;19(1):53–65. https://doi.org/10.1016/S0167-4730(96)00030-6.
[31] Rosowsky DV. Reliability-based seismic design of wood shear walls. J Struct Eng 2002;128(11):1439–53. https://doi.org/10.1061/(ASCE)0733-9445(2002)128:11(1439).
[32] Rosowsky DV. Evolution of probabilistic analysis of timber structures from second-moment reliability methods to fragility analysis. Struct Saf 2013;41:57–63. https://doi.org/10.1016/j.strusafe.2012.10.004.
[33] Saassouh B, Lounis Z. Probabilistic modeling of chloride-induced corrosion in concrete structures using first- and second-order reliability methods. Cem Concr Compos 2012;34(9):1082–93. https://doi.org/10.1016/j.cemconcomp.2012.05.001.
[34] Smith SH, Kurtis KE, Tien I. Probabilistic evaluation of concrete freeze-thaw design guidance. Mater Struct 2018;51(5):124. https://doi.org/10.1617/s11527-018-1259-z.
[35] Dolinski K. First-order second-moment approximation in reliability of structural systems: critical review and alternative approach. Struct Saf 1982;1(3):211–31. https://doi.org/10.1016/0167-4730(82)90027-3.
[36] Ellingwood BR. Structural reliability and performance-based engineering. Proc Inst Civ Eng - Struct Build 2008;161(4):199–207. https://doi.org/10.1680/stbu.2008.161.4.199.
[37] Maskey S, Guinot V. Improved first-order second moment method for uncertainty estimation in flood forecasting. Hydrol Sci J 2003;48(2):183–96. https://doi.org/10.1623/hysj.48.2.183.44692.
[38] Wong FS. First-order, second-moment methods. Comput Struct 1985;20(4):779–91. https://doi.org/10.1016/0045-7949(85)90039-2.
[39] Eu BC. A modified moment method and irreversible thermodynamics. J Chem Phys 1980;73(6):2958–69. https://doi.org/10.1063/1.440469.
[40] D. Green, J. Winandy, and D. Kretschmann, "Wood handbook: wood as an engineering material." USDA Forest Service, Forest Products Laboratory, 1999.
[41] Standard test methods for density and specific gravity (Relative density) of wood and wood-based materials. D2395. 2017.
[42] Standard test methods for small clear specimens of timber. D143. 2023.
[43] National design specification for wood construction. 2024th ed. 2024.